Soft Matter c3sm50551k

PAPER

1

Measuring the surface tension of yield stress fluids

J. Boujlel and P. Coussot

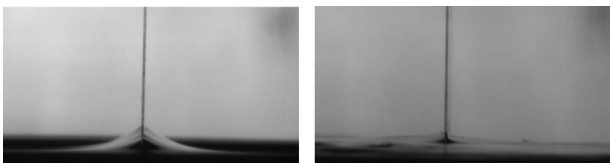

The aspect (meniscus) of an initially planar free surface put in contact with a solid blade (thickness: 0.1 mm) for (left) a simple liquid (water) and (right) a yield stress fluid (a Carbopol gel of yield stress: 40 Pa).

Queries for the attention of the authors

Journal: **Soft Matter**

Paper: **c3sm50551k**

Title: **Measuring the surface tension of yield stress fluids**

Editor's queries are marked like this...**1**, and for your convenience line numbers are inserted like this... 5

Please ensure that all queries are answered when returning your proof corrections so that publication of your article is not delayed.

Query Reference	Query	Remarks
1	For your information: You can cite this article before you receive notification of the page numbers by using the following format: (authors), Soft Matter, (year), DOI: 10.1039/c3sm50551k.	
2	Please carefully check the spelling of all author names. This is important for the correct indexing and future citation of your article. No late corrections can be made.	
3	Do you wish to indicate the corresponding author(s)?	
4	Do you wish to add an e-mail address for the corresponding author?	
5	In the sentence beginning 'Various industrial…' should 'preparation' be changed to 'utensils'?	
6	In the sentence beginning 'These materials have…' should 'interest to be' be changed to 'benefit of being'?	
7	As two versions of eqn (5) were supplied, the second version of eqn (5) has been changed to eqn (6). Please check that the renumbering is correct and that all of the citations within the text correspond to the correct equation, and indicate any changes required.	

Soft Matter

RSC Publishing

PAPER

Measuring the surface tension of yield stress fluids

J. Boujlel and P. Coussot

Cite this: DOI: 10.1039/c3sm50551k

Received 22nd February 2013
Accepted 25th April 2013

DOI: 10.1039/c3sm50551k

www.rsc.org/softmatter

With the aim of studying the impact of capillary forces on the flow of yield stress fluids we investigate the properties of a film formed by withdrawing a blade from a bath of such a material. We show that before a progressive breakage of the film, the force amplitude reaches a maximum which is independent of the initial depth of penetration and the timing for blade lifting, but increases with the material yield stress and the blade thickness. This critical force is shown to reflect both capillary and viscous effects, even at vanishing blade velocity. We demonstrate that the ratio of this force to the blade perimeter provides the surface tension of the yield stress fluid in the limit of a low ($\ll$1) capillary number (ratio of yield stress times the blade thickness to surface tension). Moreover we show that all our data for the force to perimeter ratio fall along a master curve which may be used to deduce the surface tension from measurements obtained at a capillary number up to 1, even if viscous effects are significant. Finally Carbopol gels appear to have almost the same value of surface tension whatever their yield stress, but this value is almost 10% smaller than that of pure water.

1 Introduction

Various industrial processes involve the formation of a layer of paste over a solid surface: coating of fibers with ink or paint, spreading of mortar or plaster on walls, coating glue before tile laying, application of cosmetic foams, gels or emulsions on skin, coating of desalination poultices on cultural heritage structures, covering cooking preparation with decorating foodstuffs, *etc.* The pasty materials involved are yield stress fluids, *i.e.* they flow only when they are subjected to a stress larger than a critical value otherwise they are only deformed in a finite way. A remarkable consequence of these properties is that their apparent viscosity tends towards infinity when the shear rate tends to zero. In practice this means that in contrast with simple liquids a finite force is needed to deform them even at vanishing velocity.

So far the characteristics of yield stress fluid flows along solid surfaces have generally been considered under the assumption that interfacial effects were negligible and viscous effects were dominant. The spreading of a yield stress fluid over an inclined solid plane is even used as a technique for measuring the yield stress from the critical thickness at stoppage of a wide layer.[1] Indeed, in that case the gravity stress is simply balanced by the wall shear stress which, when the fluid just stops moving, is equal to the yield stress. This balance can also be used to predict the shape of a yield stress fluid deposit formed by a progressive stoppage over an inclined plane.[2,3] The impact of wetting conditions on the flow of a yield stress fluid over a solid surface was studied only in very specific cases, *i.e.* drop impact[4–7] and thin film flows,[8] but these studies already showed that original trends can be observed when both capillary effects and the complex solid–liquid nature of these materials play a role. In contrast, for simple (Newtonian) liquids there is a well-developed background for describing thin layer spreading, coating, and wetting on solid surfaces by taking into account surface tension, viscosity and gravity effects.[9–11]

One reason for the fact that viscous effects are generally assumed to be dominant in yield stress fluid flows is that we do not have clear information about the effective surface tension of such materials. For fluids made of elements in suspension in a simple liquid, such as foams, emulsions, suspensions, and colloids, it was suggested that surface tension is simply equal to that of the interstitial liquid,[12] since all the elements (bubbles, droplets, particles, *etc.*) and in particular those situated along the fluid–air interface are generally surrounded by liquid. Actually the above physical argument might fail for concentrated systems for which the liquid layer along the interface is very thin (such as in some emulsions or foams), or when the components of the liquid layer along the air–fluid interface are unknown (such as in some concentrated pastes).

More generally the role that is played by the elements which form a network of interactions at the origin of the yield stress may be critical during surface tension measurements. Indeed let us consider, in the vein of Israelachvili's reasoning,[13] that we open a yield stress fluid sample into two parts so that we increase the area of the interface between the fluid and air. Some surface energy will generally be required for this operation. However we will also need to provide some viscous energy to strongly deform the sample at least around the region of separation. It is known that the contact angle of simple liquids

Université Paris-Est, Laboratoire Navier (UMR 8205), CNRS, ENPC, IFSTTAR, F-77420 Marne-la-Vallée, France

may be affected by non-negligible viscous effects[14–16] but this effect disappears at vanishing velocity. In contrast with simple liquids, for a yield stress fluid the viscous energy does not tend to zero for a vanishing velocity of deformation. Due to the fluid yield stress this energy tends to a finite value.

There is thus a need to develop a technique for measuring the surface tension of yield stress fluids and describe the conditions of validity of this measure. In the literature only scarce data may be found on this aspect: one study specifically focused on the measurement of surface tension of a gel from periodic laser irradiation of the surface[17] and found the value of the interstitial liquid; in their work dedicated to the determination of the elongational properties of yield stress fluids a couple of authors mentioned measurements of the surface tension of fluids exhibiting a sufficiently low yield stress,[18–20] but without much detailed information on the experimental setup, procedure, possible problems, and data. For simple liquids there exist various techniques: pendant drop, drop weight, maximum bubble pressure, Wilhelmy, du Nouy ring, *etc.* However, for the reasons above-mentioned it is likely that they cannot readily be used for yield stress fluids without great care and further analysis of the data. Indeed they are based on the measure of residual stresses at rest or at sufficiently low velocities, which correspond to situations for which there may exist finite residual stresses in the fluid.

Here we focus on the possibility of measuring the surface tension of a yield stress fluid with the help of a technique derived from the Wilhelmy technique, *i.e.* by withdrawing a film from a fluid bath. We first present the experimental setup and procedure. Then we study in detail the force variations in time during this operation in order to identify the different regimes associated with the different steps of the process. Finally we show the possibility of extracting the effective surface tension of the fluid from a series of tests by varying the experimental conditions.

2 Materials and procedures

2.1 Materials

We used simple yield stress fluids, *i.e.* solutions of Carbopol (U10) in water, whose structure is essentially that of a "glass comprised of individual elastic micro-sponges" with a typical element size of 2 to 20 μm.[21] These materials have the interest to be non-thixotropic, namely their rheological properties do not change under shear or at rest. Typically simple concentrated emulsions, foams and some physical gels appear to behave essentially as simple yield stress fluids whereas attractive colloidal systems are generally thixotropic yield stress fluids;[22] for measuring surface tension a thixotropic character might constitute an additional complexity that we will not address here.

Carbopol solutions are obtained by dispersing Carbopol (U10) powder in water. The preparation begins with a Heidolf plastic agitator being added to a glass container filled with the appropriate amount of water and set at a rate of 1000 rpm. The appropriate amount of raw Carbopol powder is then slowly added to the stirring water and allowed to incorporate. Afterwards an appropriate amount of sodium hydroxide is quickly added to the solution, elevating the pH of the acidic solution, and the agitator displaced throughout the entire container to ensure homogenous incorporation. Once incorporated the Carbopol solution is mixed for approximately 24 h in a metallic industrial mixer allowing full homogenization. Six different weight concentrations of Carbopol in the range [0.1, 0.5%] were used but since a slight variation in the procedure can lead to a significant change in the rheological properties of the final mixture here we describe these materials only through these properties, which remained constant during the experimental period.

2.2 Rheology

Rheological tests were performed with a Malvern Kinexus-stress-controlled rheometer equipped with two circular, rough plates (diameter: 6 cm). The samples were placed on the lower plate. The top plate was slowly lowered onto the sample, with great care not to entrain any air bubbles, until reaching a sample thickness of 2 mm. Excess sample was removed from the periphery. In order to minimize evaporation the sample was surrounded with a plastic cover sealed around the geometry and leaving only a minute hole at the top allowing the axis rotation.

We performed stress ramp tests, wherein the stress was increased logarithmically in time at a constant rate (for three minutes) and then decreased logarithmically in time for three minutes. The stress was followed as a function of the strain rate. The data corresponding to the decreasing shear rate range were considered as the flow curve of the material. Remark that in a parallel disk geometry the shear rate in the gap increases from zero along the central axis to a maximum at the periphery, so that a correction is required in order to obtain the effective shear rate and shear stress at the periphery (see ref. 23). We applied this correction to our data.

As already described in various previous studies these materials appear to behave as simple yield stress fluids (without thixotropy), *i.e.* solid below a yield stress (τ_c), liquid otherwise, and their flow curve, *i.e.* steady state shear stress (τ) *vs.* shear rate ($\dot{\gamma}$) data in the liquid regime, can be very well fitted (see Fig. 1) over a four decade range of shear rates [10^{-2}; 10^{2} s^{-1}] by a Herschel–Bulkley model, namely:

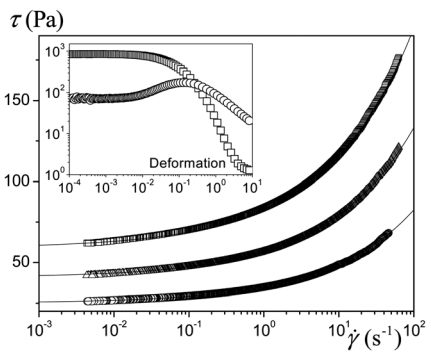

Fig. 1 Flow curves of different Carbopol solutions. The continuous lines correspond to a Herschel–Bulkley model (1) fitted to data with the following yield stress values (from bottom to top): 25, 40.7, and 59 Pa. The inset shows the elastic (squares) and loss (circles) moduli for a Carbopol solution of yield stress 80 Pa.

$$\tau < \tau_c \Rightarrow \dot{\gamma} = 0 \text{ (solid regime)} \quad (1a)$$

$$\tau > \tau_c \Rightarrow \tau = \tau_c + k\dot{\gamma}^n \text{ (liquid regime)} \quad (1b)$$

where k and n are material parameters. An example of the flow curves of different Carbopol solutions is given in Fig. 1. Note that a specificity of yield stress fluids is that their apparent viscosity ($\tau/\dot{\gamma}$) tends to infinity when the shear rate tends to zero, as may be seen from eqn (1). For such materials it was also shown from MRI measurements that this macroscopic constitutive equation effectively corresponds to their local rheological behavior.[24] For the present tests we used Carbopol solutions with yield stresses in the range 3–80 Pa. The value for n was in any case 0.38. For k we found in any case values very close to $(\tau_c/2.6)s^n$ but since, as will be demonstrated below, the second stress term in eqn (1b) plays a negligible role in our tests. For the sake of simplicity in the following we describe the Carbopol gels through the value of their yield stress only.

We also carried out oscillatory tests in order to determine the elastic and loss moduli (at a frequency of 1 Hz) as a function of the deformation amplitude. Typical data are shown in the inset of Fig. 1 for a given Carbopol solution. The elastic and loss moduli were found to be roughly proportional to the yield stress of the material.

2.3 Experimental setup for surface tension measurement

The principle of our experiment is to put a thin vertical metal blade in contact with the fluid and measure the force needed to maintain the blade at rest or to lift it from the fluid bath.

Our experimental setup is composed of a vertical blade fixed in a clamp connected in series with the top plate of a dual-column testing system (Instron model 3365) (see Fig. 2) which controls the vertical position with a resolution of 0.118 μm. The apparatus is equipped with a 10 N static load gauge able to measure the force within $\pm 10^{-6}$ of the maximum value. The container filled with fluid is fixed on the lower plate of the machine. The blade is moved vertically at a constant speed and the force needed for that is measured. The blade speed can be varied from 0.001 to 17 mm s^{-1}.

The clamp allows fine adjustment of the position (vertical and horizontal) of the blade and hence makes it possible to optimize the parallelism between the bottom of the blade and the fluid surface, an aspect which is critical to carry out well controlled measurements. In addition the angle of the container with regard to the horizontal could be adjusted finely. At last the container was equipped with a scraping system that allows us to remove the excess of fluid and, overall, to ensure the flatness of the free surface of the fluid. This system is made of a metal (steel) plate sliding along the upper edges of the container, and orientated at an angle of 45° with respect to the free surface of the fluid. The whole system is connected to the machine so as to allow a horizontal movement of the plate to be imposed at a constant speed.

For surface tension measurements we used stainless steel blades (L = 10 cm, except in one case (7 cm) which will be mentioned) with different thicknesses (E) in the range 0.1–2 mm. The blades were cleaned before each measurement. This was done by first rubbing them under water to remove any elements adsorbed on the surface and then they were cleaned with acetone and finally rinsed with distilled water.

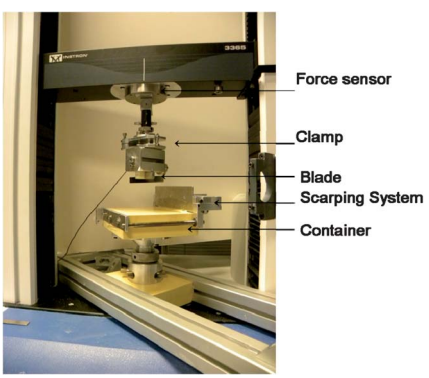

Fig. 2 The experimental setup for surface tension measurements.

2.4 Experimental procedure

Setting the blade in contact with the fluid is a critical stage of the experiment. In order to investigate force variations for very small displacements of the blade an excellent alignment between the blade and the surface of the fluid is required. Indeed any default implies that at some stage of the motion only one part of the blade will be in contact with the free surface of the fluid whereas any theoretical analysis will rely on the assumption of a complete contact. As a consequence the free surface must be as flat as possible and the blade must be approached parallel to it.

We used the following procedure. The position of the (empty) container and that of the blade are adjusted so as to be parallel. The container is filled with the fluid and, with the help of the system described above, the free surface is scraped at a constant speed (1 mm s^{-1}). The force is set to zero. Then the blade is approached into contact with the fluid at a very low speed [2–10 μm s^{-1}] while recording the force. The first contact is detected when a force jump is observed. The position of the free surface ($h = 0$) is then associated with the position reached at that time. Then the blade is slowly moved up and the force recorded in time and as a function of the current height above the level of the initial free surface (h). For some experiments the blade was first moved down through the fluid before being withdrawn. In that case the force variations were observed as a function of the depth of penetration with regard to the initial free surface, *i.e.* $-h$. All measurements were carried out at ambient temperature: 23 °C ± 1.

3 Results

3.1 First contact of the blade with the free surface of the fluid

A basic test for appreciating surface tension effects consists of putting a solid object in contact with the free surface of the fluid. When the blade enters in contact with a simple liquid this

leads to some deformation of the free surface (see Fig. 3a) associated with a slight upward displacement if the angle of contact (θ) between the two materials is smaller than 90°. When the two materials get into contact (see Fig. 4) the force on the blade suddenly drops from zero to a negative value, due to the capillary force now exerted by the liquid along the blade. This force is written as:

$$F_{Ca} = P\sigma\cos\theta \quad (2)$$

in which $P = 2(E + L)$ is the perimeter of the blade.

For a yield stress fluid we observe qualitatively the same trend (see Fig. 3b and 4), suggesting some similar capillary effects. The shape of the interface (see Fig. 3a and b) and the force (see Fig. 4) for water and a Carbopol gel of low yield stress are close, which would be consistent with the idea that the surface tension of the gel is imposed by that of the interstitial liquid. However the point here is that for the same material type, *i.e.* a Carbopol gel, but with a higher yield stress, the effect tends to disappear, *i.e.* the free surface is less deformed around the blade (see Fig. 3c), and the force now significantly departs from that measured for water (see Fig. 4). Also note that the time to reach the plateau, which for a simple liquid increases with the apparent viscosity, here increases with the yield stress.

In this approach one cannot deduce the surface tension value from the force associated with the first contact since in eqn (2) the contact angle is unknown. As a consequence it is necessary to find another technique for determining the surface tension.

3.2 Withdrawal of the blade from the fluid bath

In order to remove the impact of the contact angle one possibility is to use a method derived from the du Noüy technique which consists of slowly lifting a ring in contact with the fluid. Indeed, we can expect that by lifting the blade we will extend the film and decrease the contact angle to zero.

In that case the typical force variation for a simple liquid is shown in Fig. 5: after the sudden drop associated with the first contact ($h \approx 0$, see above) we observe a progressive decrease of the force amplitude which is due to the fact that the angle of contact is forced to tend to zero. Note that this approach is valid only if the contact line remains pinned to the blade. Then the force suddenly comes back to zero when the liquid film breaks

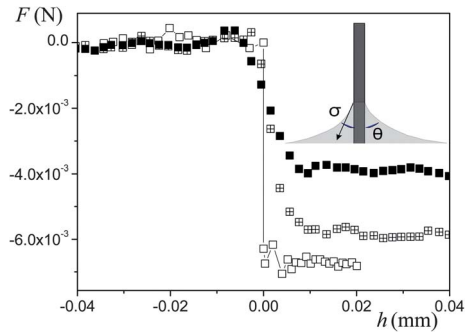

Fig. 4 Force variation around the first contact between a blade and different types of fluids: water (empty squares), Carbopol gel ($\tau_c = 5$ Pa) (cross-squares), and Carbopol gel ($\tau_c = 40$ Pa) (filled squares).

(see Fig. 5). It may be considered that film breakage occurs when the angle of contact is exactly equal to zero. Indeed, just after that time, during further withdrawal of the blade, the film thickness will become smaller below the blade tip, which is generally an unstable situation. According to eqn (2) the critical force (F_c) associated with the film breakage is thus the maximum capillary force (σP) reached for $\theta = 0$. We checked (see the inset of Fig. 5) that this technique with our specific tools effectively provides the values for the surface tension for water, glycerol and silicone oil which may be found in the literature.

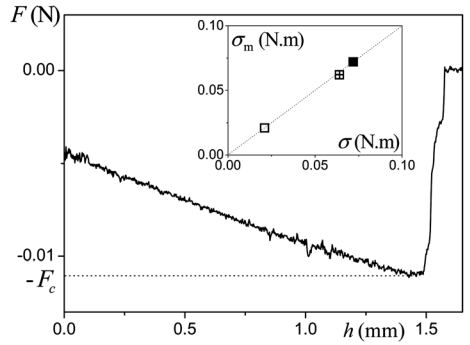

Fig. 5 Typical shape of the curve of force *vs.* distance from the initial free surface when lifting a blade initially set in contact with a bath of simple liquid. The inset shows the measured surface tension ($\sigma_m = F_c/P$) as a function of the literature value (σ) for silicone oil (empty square), glycerol (cross-square) and water (filled square).

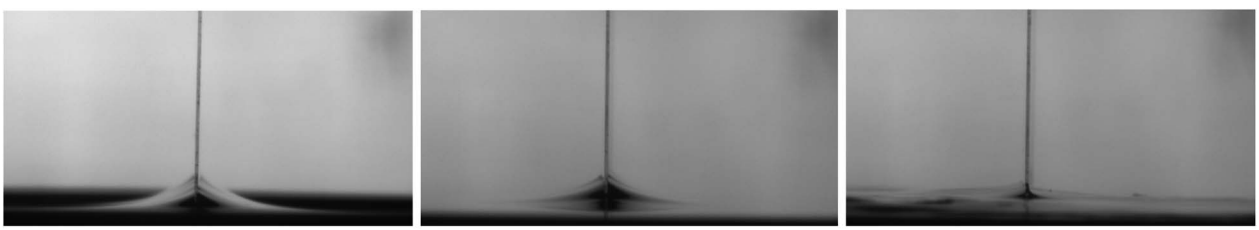

Fig. 3 Aspect (meniscus) of an initially planar free surface put in contact with a solid blade ($E = 0.1$ mm) for different fluids: (a) water, (b) Carbopol gel ($\tau_c = 5$ Pa), and (c) Carbopol gel ($\tau_c = 40$ Pa).

For a yield stress fluid, during the first stages (a), (b) and (c) (see Fig. 6) the force roughly evolves in the same way as with a simple liquid: when the blade is lifted the force progressively decreases (see Fig. 4). At some point the force reaches a minimum (stage (d)) and starts to increase (stage (e)). We remark that this increase is more progressive than for water: in the example of Fig. 4 this takes about 20 s, corresponding to an upward displacement of 2 mm. This means that the film does not break abruptly, it progressively becomes thinner. Such a result can be explained by the fact that we are here dealing with a material which is much more viscous than water.

The aspect of the film at the transition between stages (d) and (e) is shown more precisely in Fig. 7. The contact line remains pinned in its highest position so that there remains a thin layer of fluid along the plate but the film tends to be aligned with the blade direction. This means that, as for a simple liquid, the angle of contact is close to zero when the force is minimum ($-F_c$ in Fig. 6). Such a description, which relies on our direct observations and the analogy with the process with a simple liquid, is consistent with the force evolution: the total force amplitude can significantly decrease only when either (i) the viscous force, associated for example with the normal stress in the neck region, decreases because the area of the cross-section in this region decreases and/or (ii) the capillary force resulting from the film curvature significantly increases during the pinch off process.

However, considering the specificities of the mechanical behavior of the material, we need to further study the process before being able to conclude that it can effectively be used for determining the surface tension. In particular we can wonder whether the critical force depends on the procedure. For a simple liquid we know that (i) for a sufficiently slow motion viscous effects are negligible and (ii) at our scale of observation relaxation effects in the material are instantaneous. This in particular means that the blade velocity does not play any role below some critical value, no relaxation effects occur if the blade motion is stopped then restarted during the experiment, and the fluid at rest in the bath below the vertical film (region B, see Fig. 7) does not play any role.

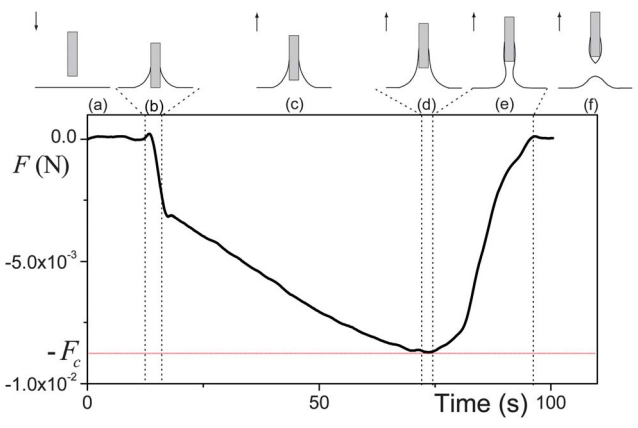

Fig. 6 Typical force *vs.* time during a sequence of descent to contact then lift until full breakage of the meniscus for a Carbopol gel ($\tau_c = 13$ Pa) (blade: $E = 0.1$ mm, $L = 70$ mm): different regimes are identified (see text) and illustrated in the above schemes.

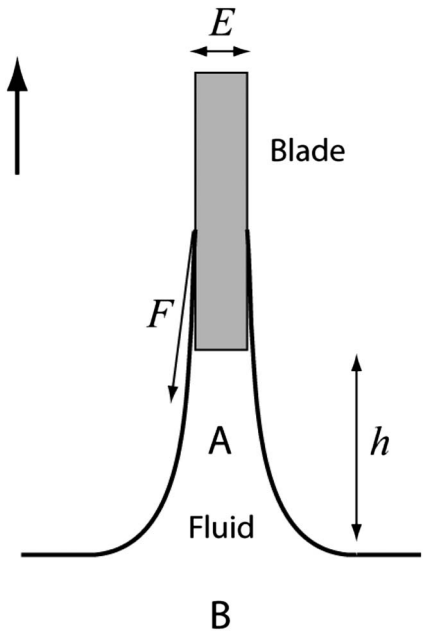

Fig. 7 Scheme of the film during blade lifting just before reaching the breakage regime.

With a yield stress fluid the situation is different: we are now dealing with a material which depending on circumstances can be either a viscoelastic solid or a liquid, so that its apparent viscosity tends to infinity at low velocity and relaxation processes can take very long times. As a consequence, as for a solid, the force on the blade might be affected by the deformation of the material which is in its solid regime far from region A (see Fig. 7). Moreover, since the material goes back to its solid state when it is left at rest for some time, one may fear that the measurements would be affected (relaxation effects) by a possible period of rest during the test. At last, since the apparent viscosity of the material tends to infinity for a vanishing velocity it is not clear whether we can effectively remove the impact of viscous effects by imposing a sufficiently slow motion. In the following we investigate these different aspects.

3.3 Impact of the procedure on the force *vs.* height curve

Impact of lifting velocity. In order to explore the role of viscous effects in the critical force before breakage we investigate the impact of the lift velocity of the blade. It appears (see Fig. 8) that the shape and position of the force *vs.* height curve are not affected by the velocity for sufficiently low velocities and F_c is constant for a velocity lower than 0.3 mm s^{-1}. For larger velocities the critical force amplitude increases. So we have a situation for which the critical force is constant then starts to increase beyond some critical velocity. This situation is typically encountered with any type of yield stress fluid flow: at low velocities the flow rate dependent term in the constitutive equation tends to zero so that the stress tends to a finite value and a critical force associated with this stress is needed to

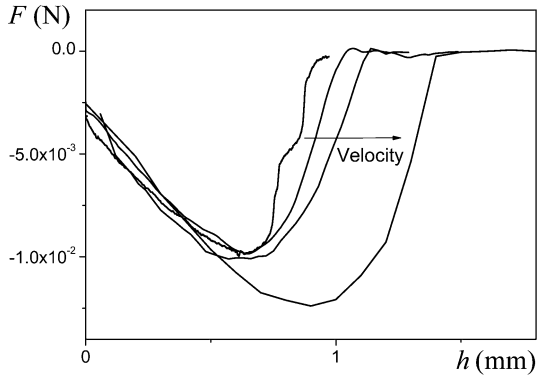

Fig. 8 Force *vs.* height when lifting the blade ($E = 0.2$ mm) in contact with a Carbopol gel ($\tau_c = 13$ Pa) for different lifting velocities: (from left to right) 0.002 mm s^{-1} and 0.1, 0.3, 1 mm s^{-1}.

induce the flow; when the velocity increases the flow rate dependent component can become significant and the force starts to increase with the velocity.

Such a trend is generally described with the help of the Bingham number, which is the ratio of the two typical stress components associated respectively with the yielding and with the additional stress beyond yielding (*i.e.* the first term to the second term of the expression (1b) for the shear stress): $\mathrm{Bi} = (\tau_c/k)(d/V)^n$, in which d is a characteristic length of the flow. This number finally expresses the ratio of the minimum viscous energy needed for flow at vanishing velocity (*i.e.* related to the yield stress) to the additional viscous energy (*i.e.* flow rate dependent component) beyond the yielding term. The flow rate dependent component is expected to be negligible for $\mathrm{Bi} \gg 1$ (*i.e.* at vanishing velocity). In contrast, the yielding term is negligible when $\mathrm{Bi} \ll 1$. Here the values for Bi (using the blade thickness for d) for the different (increasing) velocities (Fig. 8) are 17, 4, 2.5, and 1.6. This suggests that for our specific flow conditions the additional viscous component (flow rate dependent) becomes significant only when the Bingham number becomes very close to 1.

In order to avoid any possible role of the velocity dependent component, all the results presented in the following will concern situations for which the velocity is sufficiently low (Bingham larger than 5), a range in which, according to the above observations, we can rely on a single force *vs.* depth curve (independent of velocity). It is worth emphasizing that this does not mean that viscous effects are negligible. Indeed the yielding term in the constitutive equation can play a role and, in the absence of capillary effects, will definitely be at the origin of the minimum force needed to induce a flow of the material in its liquid regime at vanishing velocity.

Impact of the surrounding fluid. In order to appreciate how the deformations and flow in the regions of fluid around the region of contact play a role in the results concerning the critical force we investigate the impact of direct modification of the flow conditions on these regions. With that aim we vary the depth of penetration of the blade. We know that for simple liquids this does not affect the result, the breakage occurs always for the same critical force if the withdrawal is sufficiently slow so that viscous effects are negligible. We carried out tests by imposing some further penetration of the blade after the first contact and recorded the force *vs.* height curve.

Let us examine the force variation as a function of the height during such a test. We have already seen that when the blade is first put in contact with the fluid the force rapidly drops to a negative value associated with capillary effects. If the blade is lifted the force starts to go back to zero for some critical value of h: h_c (see Fig. 9, squares) [note that in Fig. 9 we represent the force *vs.* the depth below the initial free surface (*i.e.* $-h$)]. If instead the blade is pushed further downwards the force first starts to increase from the value it had reached after the first contact (see Fig. 9, continuous lines). This situation has been studied in detail recently:[23] the force first results from some elastic deformation of the surrounding fluid in its solid regime, then from an almost uniform flow in the liquid regime along the sides of the blade. This means that after some distance of penetration the additional stress along the blade for further penetration is that associated with this uniform viscous flow and the buoyancy force, which in particular explains that the force increases linearly with the depth of penetration (see Fig. 9).

At some depth we start to impose an upward motion to the blade. The force then abruptly starts to decrease (see Fig. 9) and finally reaches a kind of plateau (slightly inclined). At the end of this plateau the force suddenly starts again to increase and reaches zero exactly in the same way as without the penetration process: the curves associated with different penetration depths superimpose along the plateau and during the final film separation process (see Fig. 9). Even more striking is that in this region the curves are similar to the data without any penetration (see Fig. 9). Thus the critical force measured with or without penetration is the same and we can conclude that the residual force before film breakage is not affected by the flow of the surrounding fluid.

Note that the above result is valid only if the depth of penetration is sufficiently small, otherwise the mass of material stuck along the sides of the blade lifted above the fluid induces

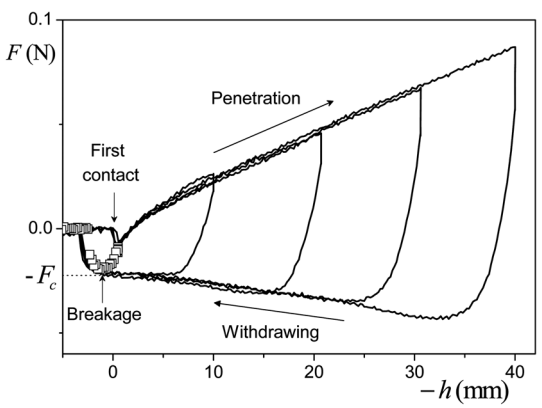

Fig. 9 Force as a function of depth below the initial free surface for a downward motion followed by an upward motion of the blade ($E = 0.5$ mm, $L = 100$ mm) in a Carbopol gel ($\tau_c = 3$ Pa) with different maximum depths of penetration: 0 mm (squares) and from left to right 10, 20, 30 and 40 mm (continuous curves).

a significant additional component during withdrawal. In the example shown in Fig. 9 this was clearly not the case since one can see that the force level after film breakage, which is essentially equal to the weight of material stuck on the plate sides, is independent of the maximum depth of penetration. In the general case, if the plate is pushed at some significant depth through the fluid before withdrawing it may be necessary to take into account the amount of fluid stuck along the plate sides, which can be done by considering that this simply leads to an additional force term (in the critical force) equal to the weight of fluid stuck measured *via* the residual force after breakage.

Impact of relaxation effects. In order to investigate the possible impact of relaxation effects on our measurements with these complex fluids we carried out tests by adding a time of rest between the first contact of the blade with the free surface and the blade lifting. During the rest period the force level is not always the same and the force can slowly drift but anyway, its variations as soon as the lifting starts are similar for any time of rest [<10 min]: the force first decreases when the film is elongated then decreases when it progressively breaks. Finally the critical force is approximately the same for different times of rest. We conclude that even if there are some relaxation effects during the rest period the force variation during the lifting phase is similar so that, for such a simple (non-thixotropic) yield stress fluid, the previous relaxation processes do not have any impact on the determination of the critical force.

We also looked at the impact of some stoppage during the lifting motion before breakage (Fig. 6, stage c). As shown in Fig. 10 such a procedure does not affect the result concerning the critical force: the blade is stopped for two different periods during the lifting process; during these periods the force keeps a constant value then starts again to decrease when the motion starts again. As a consequence the force *vs.* height variations with or without stoppage periods are similar (see the inset of Fig. 10) and the critical force is independent of the exact timing for lifting the blade. These results in particular prove that when removing the blade from the bath, the contact line remains anchored on the blade, otherwise a wall slip in the process during the stoppage periods would lead to different data for different withdrawal timings. This supports our hypothesis that the contact line position along the blade remains fixed and only the contact angle decreases during the withdrawal phase (stage c in Fig. 6).

Note that during the breakage phase things might be more complex. Viscous effects also no doubt play a significant role, but the relaxation of a plate moving then stopped in a similar yield stress fluid[23] was shown to occur over a time-scale (typically 25 s) similar to that for the breakage phase observed here. This suggests that both viscous and relaxation effects could play some role during the breakage phase but as yet we cannot reach a definitive conclusion.

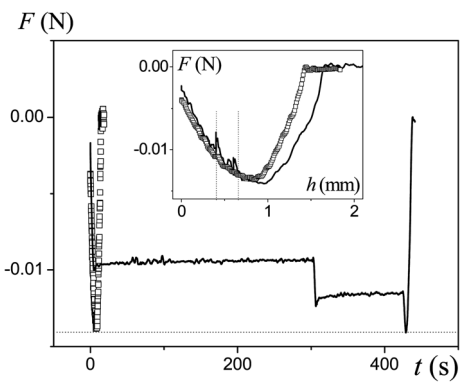

Fig. 10 Force *vs.* time during blade withdrawing from a Carbopol gel ($\tau_c = 25$ Pa, $E = 0.2$ mm) without (squares) or with (continuous line) stoppage periods (leading to two force plateaus). The inset shows the corresponding force *vs.* height variations.

4 Discussion

4.1 Generalities

From the above results we deduce that the critical force on the blade before separation does not depend on the flow history in the fluid bath below the vertical film. This suggests that this critical force is essentially due to the deformation and/or flow in this vertical film. Moreover we have seen that the critical force is unaffected by a period of rest during lifting and does not depend on the velocity when it is sufficiently low. This means that we are always just beyond the transition between the solid and the liquid regime, *i.e.* the plastic regime, and during a period of rest the residual stresses in the fluid are maintained at the level they have just before the solid–liquid transition.

Finally we expect to have a critical force related to the flow characteristics of the material in the vertical film (region A in Fig. 7) with the following effects potentially playing a role:

- capillary effects, as in the case of a simple liquid, with a surface tension σ;

- viscous effects, associated with the flow of the film in its plastic regime;

- gravity effects.

If we assume that the surface tension of the fluids does not vary with the concentration, capillary effects should have a constant impact on the critical force whatever the yield stress value and the blade thickness (as long as it is small compared to the blade width). The force associated with viscous effects in the plastic regime is expected to be proportional to the material yield stress and to the section of the fluid film, which is proportional to the blade thickness. At last the force associated with gravity effects is proportional to the volume of material in the film, which for a given height is proportional to the blade thickness.

In order to observe the effect of the main parameters on the data we varied the thickness and the yield stress of the materials and looked at the variations of the *apparent surface tension*, *i.e.* $f = F_c/P \approx F_c/2L$ (see Fig. 11). It appears that f increases with the thickness for all yield stress values but for the smallest yield stress values there seems to be a plateau at small thickness, as if the apparent surface tension tended to saturate. Besides f increases with the yield stress as appears from the global increase of the level of the different curves, but the shape does not seem to be exactly the same for different values. This

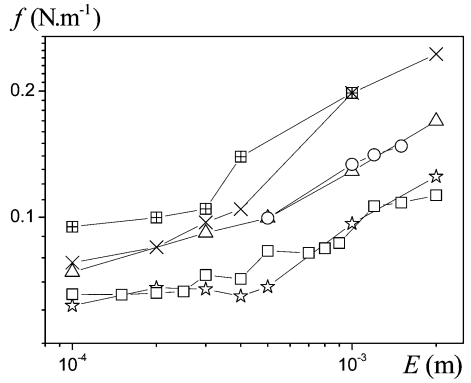

Fig. 11 Apparent surface tension as a function of the blade thickness for Carbopol gels with different yield stresses: 9 Pa (squares), 13 Pa (stars), 25 Pa (triangles), 35 Pa (circles), 75 (cross-squares), and 80 Pa (crosses).

suggests that both the viscous effects and the gravity effects can have an impact on the apparent surface tension. In order to further analyze the data it becomes clear that we need to develop a more precise theoretical approach.

4.2 Theoretical analysis

Let us consider the complete flow characteristics of the fluid film which forms below the blade during lifting. As a first approximation we can assume that when the force reaches the critical value the shape of the film is such that it essentially undergoes an extensional flow. In order to describe this flow type the constitutive equation in simple shear eqn (1) is not sufficient, we need a tensorial expression. The complete (tensorial) representation of the rheological behavior of a simple yield stress fluid such as the Carbopol gel is usually directly extrapolated from the simple shear behavior (*i.e.* eqn (1)) in the following form:[12]

$$\sqrt{-T_{\mathrm{II}}} < \tau_c \Rightarrow \boldsymbol{D} = 0 \quad \text{(solid regime)} \tag{3a}$$

$$\sqrt{-T_{\mathrm{II}}} > \tau_c \Rightarrow \boldsymbol{\Sigma} = -p\boldsymbol{I} + \boldsymbol{T} = -p\boldsymbol{I} + F(D_{\mathrm{II}})\boldsymbol{D} + \tau_c \boldsymbol{D}/\sqrt{-D_{\mathrm{II}}} \quad \text{(liquid regime)} \tag{3b}$$

in which $\boldsymbol{D}$ and $\boldsymbol{\Sigma}$ are respectively the strain rate (symmetric parts of the velocity gradient tensor) and stress tensors, p the pressure, $\boldsymbol{I}$ the unit tensor, $\boldsymbol{T}$ the extra-stress tensor, $T_{\mathrm{II}} = -\mathrm{tr}(\boldsymbol{T})^2/2$ and $D_{\mathrm{II}} = -\mathrm{tr}\boldsymbol{D}^2/2$ the second invariants of the stress and strain rate tensors, and F is a function such that: $F(D_{\mathrm{II}}) = 2^n k/\left(\sqrt{-D_{\mathrm{II}}}\right)^{1-n}$. In the above expressions the three rheological parameters, τ_c, k and n, can be determined from simple shear experiments since in that case the constitutive equation leads to an equation of the form eqn (1).

Now we assume that when we approach the critical force the film below the blade is a uniform sheet of thickness e (along the axis $\boldsymbol{x}$) which decreases uniformly while its height h (along the axis $\boldsymbol{z}$) increases during blade lifting at a velocity V. The width (along the axis $\boldsymbol{y}$) of the film is supposed to remain constant. Under these conditions we are dealing with a so-called planar elongational flow for which the velocity field is expressed as follows: $v_x = -Kx$; $v_z = Kz$, in which $K = -V/h$ is the rate at which the fluid is strained ($K > 0$). Note that here we assumed that the origin ($x = y = z = 0$) is situated in the middle of the sheet. Now we can compute $\sqrt{-D_{\mathrm{II}}}$ which is found to be equal to K. Thus, from the above constitutive equation we find that if the velocity dependent component is negligible the (normal) viscous stress along the direction $\boldsymbol{z}$ is equal to the yield stress τ_c.

Let us now compute the total force acting on the blade when the film thickness has reached the blade thickness. From the above calculations we deduce that the viscous force needed to induce a further elongation of the film at that time can be expressed as $\tau_c EL$. The energy needed for a small elongation of the film and associated with a vertical displacement of dh is by definition the surface tension times the increase of the air–paste interface, *i.e.* $\sigma(2Ldh)$, which implies that the capillary force is $2\sigma L$. The gravity force corresponds to the weight of material in the film, *i.e.* $\rho gELh_c$. The total force applied on the blade at the critical point is thus:

$$F_c = 2\sigma L + \tau_c EL + \rho gELh_c \tag{4}$$

Finally the apparent surface tension under these conditions may be expressed as:

$$f/\sigma_0 = x + (1 + G)\mathrm{Ca_Y} \tag{5}$$

in which $x = \sigma/\sigma_0$, $G = \rho gh_c/\tau_c$ and $\mathrm{Ca_Y} = \tau_c E/2\sigma_0$ (where σ_0 is a surface tension of reference).

G is a dimensionless number which is often used to describe the free surface flow of a yield stress fluid, using in that case for h the thickness of the film of material over the solid surface. In the absence of inertia effects a flow is generally obtained only if G is larger than 1.[3] This means that for our tests it is essential that $G < 1$ otherwise gravity might have an effect not only on the measurement of the critical force (through eqn (4)) but also on the flow characteristics during film formation.

$\mathrm{Ca_Y}$ is a capillary number for yield stress fluids. From eqn (5) we deduce that the apparent surface tension will tend to the effective surface tension of the paste when $\mathrm{Ca_Y}$ tends to zero, *i.e.* when the yield stress times the film thickness is much lower than surface tension.

4.3 Comparison of experimental data with theory

In our case the height at breakage is around 1 mm so that G decreases from 1, for the smallest yield stress used, to 0.1 for the largest yield stress. As a consequence G does not play the major role in the result. Plotting all our data in a f/σ_0 *vs.* $(1 + G)\mathrm{Ca_Y}$ diagram (see Fig. 12) we see that they fall rather well along a single master curve with a maximum error of 20%. This result proves several points.

(1) The above theoretical analysis is globally valid and in particular we have effectively identified the main force components leading to the appropriate scalings.

(2) We can effectively identify the effective surface tension of the fluid from the plateau of the apparent surface tension

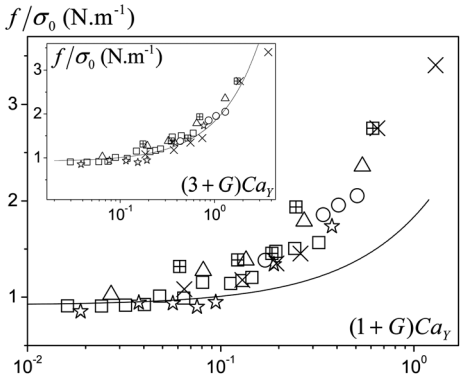

Fig. 12 Apparent surface tension scaled by the surface tension of water ($\sigma_0 = 0.072$ N m^{-1}) as a function of the capillary number for yield stress fluid (see text) times a gravity factor, for different blade thicknesses and for different Carbopol gels: 9 Pa (squares), 13 Pa (stars), 25 Pa (triangles), 35 Pa (circles), 75 Pa (cross-squares), and 80 Pa (crosses). The dotted line corresponds to eqn (5) with $x = 0.91$. The inset shows the same data represented as a function of the capillary number times a different factor. The continuous line corresponds to the empirical model described in the text.

obtained for $Ca_Y \rightarrow 0$ and which corresponds to negligible gravity and viscous effects.

(3) The surface tension of Carbopol solutions varies negligibly with the concentration, and is slightly smaller than that of water, *i.e.* $\sigma = 0.066$ N m^{-1}.

Despite this global agreement with theory the data for $Ca_Y > 0.1$ appear to fall along a curve which does not correspond to eqn (5). This difference could be explained by a difference in the viscous force. In the literature there precisely appears to remain some ambiguity on the effective value of the viscous force associated with the elongational flow of a yield stress fluid. Only a few studies have addressed this problem and strictly for a cylindrical drop of fluid. The theoretical studies essentially focused on the breakage timing.[25,26] The second of these studies[26] provided a further insight into the shape of the drop during separation, which in particular explains the final conical shape of the deposits obtained in such tests. Two other studies were specifically aimed at determining the critical force of separation from either drop elongation using a Capillary Breakup Elongational Rheometer (CaBER),[20] or drop formation and fall from a die exit.[19] In each case the measure relies on the critical force at breakage, which is supposed to be balanced by the capillary effect. A uniaxial elongational flow is assumed in the fluid around the region of breakage. In that case the theory for a simple uniaxial elongation and using a constitutive equation of the form eqn (3) predicts a normal force due to viscous effects (in the limit of large Bi) equal to $\sqrt{3}\tau_c$ times the cross-section of the fluid cylinder. In the first case,[20] with emulsions, the normal viscous force was found to be larger by a factor of 2.8 whereas in the second case,[19] with Carbopol gels, the correct theoretical factor (*i.e.* 1) was found. Recently a more complete study of the Laplace pressure in filaments[27] of various types of yield stress fluids has led to the conclusion that the yield stress factor is equal to 1 only if the measurement is taken at a ratio of the filament life time to fluid relaxation time equal to 1. In our case we can well represent the data with the equation $f = \sigma[1 + (3 + G)Ca_Y]$ (see the inset of Fig. 12), which would correspond to a viscous coefficient equal to 3. There is a need to clarify this problem.

4.4 Direct determination of the viscous term

In order to attempt to clarify the situation we carried out a series of tests using the same equipment as above now equipped with two parallel plates. We put a small droplet of fluid over the first plate and move down the upper plate so as to slightly squeeze the droplet until it forms a cylinder of aspect ratio around 1. Then we move up the upper plate at constant speed (50 μm s^{-1}) and follow the force *vs.* time. We tested different solutions of Carbopol always starting from the same initial volume of the drop. A typical curve obtained under these conditions is shown in Fig. 13. From the images of the drop shape in time we could determine the radius of curvature of the neck (R') and the radius of the minimum cross-section in the sample (R). Using the surface tension value determined above we can compute the capillary force in this fluid region, *i.e.* $\sigma(1/R + 1/R')S$, in which S is the cross-section area (note that R' is negative). The force which needs to be applied to the plate may be written as the sum of this capillary force, the viscous force, and the gravity force on the material which is lifted. We can consider that the mass of material effectively lifted during all the process is well approximated by the mass remaining stuck to the upper plate at the end of the test. The gravity force on this mass can easily be determined: it corresponds to the residual force after breakage.

Finally, in contrast with previous studies, which focused on the breakage, we can compute the normal viscous force all along the extension process. The corresponding stress for different yield stress fluids is represented in the inset of Fig. 13. The stress increases in a first period then reaches a kind of plateau. Such a shape is reminiscent of the typical stress *vs.* time curve when a low shear rate is imposed to a yield stress fluid in simple shear. The initial increase is associated with the

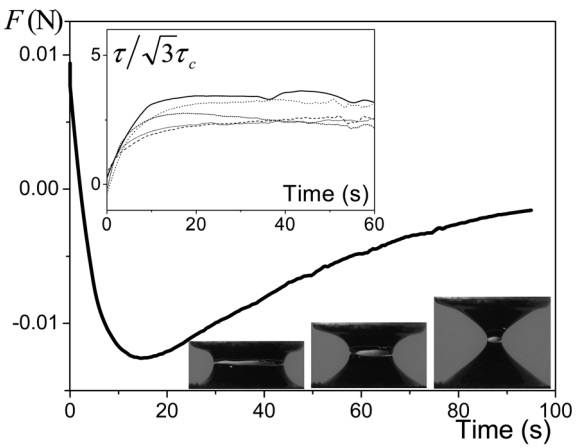

Fig. 13 Typical force *vs.* time curve during the separation of two plates in contact with a drop of yield stress fluid (a Carbopol gel, yield stress: 34 Pa). The photos show the evolution of the shape of the drop in time. The inset shows the normal viscous stress (see text) scaled by the yield stress for tests with Carbopol gels of different yield stress values: 23 Pa (continuous line), 34 Pa (dotted line), 48 Pa (dashed line), 71 Pa (short dash), and 78 Pa (short dots).

deformation of the material in its solid regime and the plateau is reached when the material has reached its liquid regime. Thus, here we can use the stress level at the plateau as the normal stress in the neck region during all the process as soon as the material effectively flows in its liquid regime.

When the normal stress curves are rescaled by the yield stress we find approximately a master curve (see the inset of Fig. 13). This means that the viscous stress is simply equal to the yield stress times a constant factor, here around 3. This value is close to the value (*i.e.* 2.8) found from the critical stress at breakage in a similar geometry.[20] It has been suggested[20] that the discrepancy between the theory and experiments concerning this problem is due to the fact that the effective constitutive equation as given by eqn (3) should also include a term depending on the third invariant of the stress tensor. This is a possibility which nevertheless does not explain the consistency found for Carbopol gels.[19,25]

Looking at the drop deformation in time (see photos in Fig. 13) leads us to suggest another explanation for this discrepancy. We could observe that as the drop is elongated an increasing fraction of the sample, in contact with the upper and lower plates, stops flowing. This phenomenon is at the origin of the conical shape of the deposits at the end of the test, which is related to the yielding and strong shear-thinning character of these yield stress fluids which may flow much more rapidly in regions of slightly larger stresses. This means that the flow progressively occurs only in a small central region, the thickness and diameter of which continuously decrease. As a consequence it is not so clear that we have a simple uniaxial elongation in this region. There might also be some shear and we know that for a squeeze flow in the lubricational regime (small thickness (b) to diameter ratio) the normal stress due to flow is equal to $\tau_c R/3b$. Thus, depending on the value of R/b this stress can be quite different from that obtained under the assumption of a uniaxial elongation. In particular it can be significantly larger if the flow is restricted to a thin layer $b \ll R$. The situation is likely different for drop formation due to the exit through the die as in ref. 19 and 25 since in that case an extension is the natural process induced by gravity. In contrast to the drop breakage between two plates the contact of the fluid with the plates tends to fix the drop diameter at a short distance from the region of breakage.

It is likely that during our film breakage a similar effect occurs, leading to a normal viscous stress higher than expected from a theory assuming a planar elongation. The above theoretical considerations show the difficulty to predict the exact value of the stress factor. However the interesting point is that in our tests there is a good consistency between the viscous factor found from the film extension and from the droplet extension tests. This leads us to conclude although we cannot yet fully explain the exact shape of the experimental master curve for $Ca_Y > 0.1$, it can be well represented by the above theory with a viscous factor of 3.

5 Conclusion

With the aim of studying the impact of capillary forces on the flow of yield stress fluids we investigated the properties of a film formed by withdrawing a blade from a bath of such a material. We showed that before progressive breakage of the film due to the high viscosity of the fluid, the force amplitude reaches a maximum which is independent of the initial depth of penetration and the timing for blade lifting, but increases with the material yield stress and the blade thickness. This critical force is shown to reflect both capillary and viscous effects, even at vanishing blade velocity. Plotting the apparent surface tension (ratio of critical force to blade perimeter) as a function of the capillary number (ratio of yield stress times the blade thickness to a reference surface tension) it appears that all the data fall along a master curve.

Although we could not fully explain the origin of this curve at the capillary number of the order or larger than 1 because the viscous contribution depends on the flow characteristics around the region of breakage which are somewhat complex, this experimental master curve provides a fundamental basis for analyzing data obtained from such tests. Indeed the plateau at low capillary number (much smaller than 1) directly provides the surface tension of the yield stress fluid. If the measurements are carried out at larger capillary number it is still possible to deduce the effective surface tension from this curve even if viscous effects are not negligible. Finally the general expression for the surface tension of the yield stress can be extracted from the following equation deduced from the empirical model fitted to our experimental data:

$$\sigma = \frac{F_c}{P} - 1.5\tau_c E - 0.5\rho g h_c E \qquad (6)$$

in which nevertheless the factor 1.5 has as yet no clear theoretical interpretation.

Note that it is preferable to use this technique only when the second term of the right hand-side of eqn (6) is not close to the first term, *i.e.* when the viscous force is not much larger than the surface tension component, otherwise the uncertainty on the measurement becomes too large. We can consider that the limit of validity of the technique is $Ca_Y < 1$. This implies that with a blade thickness of 0.1 mm it is possible to measure the surface tension of fluids exhibiting a yield stress up to several hundreds of Pascals (when the surface tension is of the order of that of water).

References

1 T. L. H. Nguyen, N. Roussel and P. Coussot, *Cem. Concr. Res.*, 2006, **36**, 1789.
2 N. J. Balmforth, R. V. Craster, A. C. Rust and R. Sassi, *J. Non-Newtonian Fluid Mech.*, 2006, **139**, 103.
3 P. Coussot, S. Proust and C. Ancey, *J. Non-Newtonian Fluid Mech.*, 1996, **66**, 55.
4 S. Nigen, *Atomization Sprays*, 2005, **15**, 103.
5 L. H. Luu and Y. Forterre, *J. Fluid Mech.*, 2009, **632**, 301.
6 G. German and V. Bertola, *Colloids Surf., A*, 2010, **366**, 18.
7 E. Kim and J. Baek, *J. Non-Newtonian Fluid Mech.*, 2012, **173**, 62.
8 N. Balmforth, S. Ghadge and T. Myers, *J. Non-Newtonian Fluid Mech.*, 2007, **142**, 143.

9 D. Quéré and A. de Ryck, *Ann. Phys.*, 1998, **23**, 1.
10 D. Quéré, *Annu. Rev. Fluid Mech.*, 1999, **31**, 347.
11 D. Quéré, P. G. de Gennes and F. Brochart-Wyart, *Capillarity and Wetting Phenomena: Drops, Bubbles, Pearls, Waves*, Springer, Berlin, 2003.
12 P. Coussot, *Rheometry of pastes, suspensions and granular materials*, Wiley, New York, 2005.
13 J. N. Israelachvili, *Intermolecular and surface forces*, Academic Press, Amsterdam, 2001.
14 E. Ramé and S. Garoff, *J. Colloid Interface Sci.*, 1996, **177**, 243.
15 G. Giannotta, M. Morra, F. Occhiello, F. Garbassi, L. Nicolais and A. Damore, *Polym. Compos.*, 1993, **14**, 224.
16 M. Morra, E. Occhiello and F. Garbassi, *J. Adhes. Sci. Technol.*, 1992, **6**, 653.
17 Y. Yoshitake, S. Mitani, K. Salai and K. Takagi, *Phys. Rev. E: Stat., Nonlinear, Soft Matter Phys.*, 2008, **78**, 041405.
18 G. German and V. Bertola, *J. Non-Newtonian Fluid Mech.*, 2010, **165**, 825.
19 G. German and V. Bertola, *Phys. Fluids*, 2010, **22**, 033101.
20 K. Niedzwiedz, H. Buggisch and N. Willenbacher, *Rheol. Acta*, 2011, **49**, 1103.
21 J. M. Piau, *J. Non-Newtonian Fluid Mech.*, 2007, **144**, 1.
22 P. Coussot and G. Ovarlez, *Eur. Phys. J. E*, 2010, **33**, 183.
23 J. Boujlel and P. Coussot, *Rheol. Acta*, 2012, **51**, 1.
24 P. Coussot, L. Tocquer, C. Lanos and G. Ovarlez, *J. Non-Newtonian Fluid Mech.*, 2009, **158**, 85.
25 P. Coussot and F. Gaulard, *Phys. Rev. E: Stat., Nonlinear, Soft Matter Phys.*, 2005, **72**, 031409.
26 N. J. Balmforth, N. Dubash and A. C. Slim, *J. Non-Newtonian Fluid Mech.*, 2010, **165**, 1147.
27 L. Martinie, H. Buggisch and N. Willenbacher, *J. Rheol.*, 2013, **57**, 627.